C. R. Physique 16 (2015) 540–552

Contents lists available at ScienceDirect

Comptes Rendus Physique

www.sciencedirect.com

The measurement of time / La mesure du temps

The ACES/PHARAO space mission

La mission spatiale ACES/Pharao

Philippe Laurent [a], Didier Massonnet [b], Luigi Cacciapuoti [c], Christophe Salomon [d,*]

[a] *SYRTE, CNRS UMR 8630, Observatoire de Paris, LNE, UPMC, 61, avenue de l'Observatoire, 75014 Paris, France*
[b] *CNES, Centre spatial de Toulouse, 18, avenue Édouard–Belin, 31401, Toulouse, France*
[c] *European Space Agency, ESTEC, Noordwijk, ZH 2200 AG, The Netherlands*
[d] *Laboratoire Kastler–Brossel, ENS–PSL Research University, CNRS, UPMC, Collège de France, 24, rue Lhomond, 75005 Paris, France*

ARTICLE INFO

Article history:
Available online 29 May 2015

Keywords:
Clocks
Cold atoms
Relativité
Precision measurements
Variation of the fundamental constants
Time–frequency transfer

Mots-clés :
Horloges
Atomes froids
Relativité
Mesures de précision
Variation des constantes fondamentales
Transfert de temps et de fréquences

ABSTRACT

Proposed in 1997, the ACES/PHARAO experiment is a space mission in fundamental physics with two atomic clocks on the International Space Station, a network of ultra-stable clocks on the ground, and space-to-ground time transfer systems. The ACES flight instruments are near completion and launch in space is planned for the first half of 2017 for a mission duration of three years. A key element of the satellite payload is a cold-atom clock designed for microgravity environment, PHARAO, operating with laser-cooled cesium atoms. Here we first report on the design and tests of the PHARAO flight model, which is now completed and ready for launch. We then briefly present the status of development of the other instruments of the ACES payload, the Space Hydrogen Maser, the microwave time-transfer system (MWL), and the laser time transfer ELT.

RÉSUMÉ

Proposée en 1997, l'expérience ACES/Pharao est une mission spatiale en physique fondamentale avec deux horloges atomiques sur la Station spatiale internationale, un réseau d'horloges ultra-stables à terre et de systèmes de transfert de temps de l'espace jusqu'au sol. Les instruments de vol ACES sont proches de l'aboutissement et leur lancement dans l'espace est planifié pour la première moitié de 2017 pour une durée de mission de trois ans. Un élément-clé de la charge utile du satellite est une horloge atomique à atomes froids conçue pour la microgravité, Pharao, qui fonctionne avec des atomes de césium refroidis par laser. Nous commençons par décrire la conception et les essais du modèle de vol Pharao, qui est maintenant opérationnel et prêt pour le lancement. Nous présentons ensuite brièvement l'état de développement des autres instruments de la plateforme ACES, le maser passif à hydrogène, le système de transfert de temps par liaisons micro-ondes (MWL) et le transfert de temps par lien laser (ELT).

* Corresponding author.
E-mail address: salomon@lkb.ens.fr (C. Salomon).

http://dx.doi.org/10.1016/j.crhy.2015.05.002
1631-0705/

1. The ACES mission

Ultracold atoms have become essential tools in modern precision measurements of space-time. Using matter-wave interferometers, local accelerations, gradients of accelerations, and rotations are measured with very high precision, see for instance [1,2]. The measurement of time using atomic clocks has also experienced spectacular progress in the recent years. Both atomic clocks and matter-wave interferometers use quantum mechanical interference between internal or external degrees of freedom to perform very sensitive phase measurements, and, as shown in [3], interferometers and clocks belong to the same class of "quantum sensors". For these sensors, the space environment is very attractive as it offers the possibility to considerably increase the coherent interaction time between electromagnetic fields and freely propagating ultracold matter-waves in well-controlled conditions.

Preliminary demonstrations of cold atom production in reduced gravity [4] and of the operation of a laser-cooled cesium clock in jet plane parabolic flights [5] were followed by atom interferometry in parabolic flights [6], Bose–Einstein condensation in free fall [7] and matter-wave interferometry with large interaction times in a ∼10-m tower [8], and in a free-fall tower [9]. All these experiments prepared the science and technology for bringing these instruments from ground-based operation into micro-gravity conditions to advance the frontier of precision measurements, tests in fundamental physics, and other applications in navigation and geodesy.

The ACES mission (Atomic Clock Ensemble in Space) was proposed to the European Space Agency (ESA) and the French Space Agency (CNES) in 1997 with the goal of operating a laser-cooled cesium primary clock in space and exploit its performance for fundamental physics tests [5,10]. The offered flight opportunity was a payload with a volume of about 1 m^3 outside the International Space Station (ISS), attached to a balcony of the European module, Columbus, which was launched in 2008 to the ISS. The ISS has a nearly circular orbit around the Earth at a mean elevation of 400 km s with an orbital period of 5400 s and an inclination of 51.6 degrees. The ACES scientific objectives have four main components, the operation of a laser-cooled cesium primary standard in space, a precision measurement of the Einstein effect, the gravitational shift of the clock frequency predicted by General Relativity, tests of Lorentz invariance, and a search for time or spatial variations of fundamental physical constants by long-distance clock comparisons.

More quantitatively, the primary ACES scientific objectives are:

- to demonstrate the performance of the cold-atom clock PHARAO in microgravity environment. The expected frequency stability of the cesium clock in space is $1{\cdot}10^{-13}\tau^{-1/2}$ for $1\ \mathrm{s} < \tau < 10^6$ s and accuracy below $3{\cdot}10^{-16}$;
- to demonstrate the performance of an active hydrogen maser in space with a stability of 10^{-13} at 1 s, down to $1.5{\cdot}10^{-15}$ at 10 000 s;
- to perform high-resolution space-ground and ground-ground time and frequency transfer in the microwave domain. The link stability should reach around 0.3 ps after 300 s of integration time and less than 6 ps after 1 to 10 days of integration;
- to perform high-resolution space-ground time transfer using an optical link with 50-ps accuracy and 5-ps stability;
- to perform a test of the gravitational red shift with 2 ppm accuracy;
- to test Lorentz Invariance (LI) in the Robertson–Mansouri–Sexel framework and Standard Model Extension (SME) [11];
- to search for time variations of fundamental constants by global clock comparisons with a sensitivity of 10^{-17} per year.

These mission objectives were previously detailed in [12–15] and are also discussed in [37] and [30]. Here we only summarize the main aspects and present the current status of development of the ACES mission elements.

2. The ACES flight payload

Fig. 1 presents a schematic view of the flight elements. The payload contains two high-precision atomic clocks. PHARAO, a cesium primary frequency standard, operates with atoms that are cooled to 1 μK, corresponding to an *rms* velocity of 7 mm/s. Its design is optimized for operating in micro-gravity environment. SHM, an active (space) hydrogen maser, serves as a phase-preserving reference oscillator with very good short- and medium-term stability. The signals of the two clocks are combined to benefit from the SHM stability in the short term and the PHARAO clock stability on the long term, i.e. above 2000 s, to provide an optimized onboard time scale. These two clocks will be compared to ground clocks operating in the microwave or optical domain using a microwave two-way time-transfer system (MWL) operating in the Ku band as well as a laser time-transfer system ELT. Because of the low orbit of the ISS, a time-transfer session with a ground receiver/emitter will last on average 400 s and can be repeated about 4–6 times per day. Therefore, it is important to perform phase-preserving successive time-transfer sessions in order to reach a precision in time scale comparisons of a few picoseconds and frequency comparisons down to the $1{\cdot}10^{-17}$ range after a few days of averaging. Over a single ISS path, the MWL specification corresponds to a time instability of 0.3 ps, increasing to 5 ps per day and 7 ps at 10 days. The company Airbus Defence and Space (ADS) is the prime contractor for this flight payload. It is responsible for the overall integration, tests, and operation of the ACES ensemble mounted on a temperature-regulated base plate with typical stability of 1 degree Celsius. Launch will be provided by NASA using a Space X rocket in the first half of 2017. The planned mission duration is 18 months, with a potential extension to 3 years.

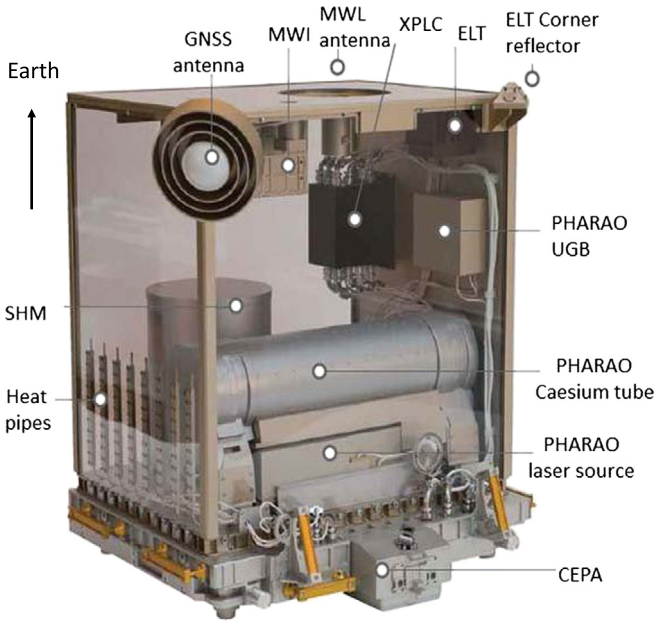

Fig. 1. (Color online.) The ACES payload. In a volume of about 1 m^3, a mass of 227 kg, and with a power of 450 W, the ACES payload will be attached on a balcony of the Columbus module of the International Space Station. The main hardware includes two high-stability atomic clocks, a laser-cooled cesium clock, PHARAO, and a hydrogen Maser SHM. Two time-transfer systems operating in the microwave domain, MWL, or with laser pulses in the optical domain, ELT, enable high-precision comparisons between the onboard timescale and timescales realized in a network of ground institutes over four continents. The orbit of the space clocks is determined with a GPS/GNSS receiver on the ACES payload. The onboard computer XPLC enables communication between the instruments and ground operations through the ISS data communication channel.

3. The network of ground clocks

Currently the network of ground institutes participating in the ACES mission with a microwave link terminal includes two institutes in the USA, JPL (Pasadena, CA), and NIST (Boulder, CO), three institutes in Europe, SYRTE (Paris, FR), PTB (Braunschweig, DE), and NPL (Teddington, UK), three institutes in the Tokyo area, Japan, NICT, NMIJ and RIKEN, connected via fiber links to one MWL terminal located at NICT, and one institute in the southern hemisphere at UWA, Perth, Australia. Furthermore, one transportable MWL station will be located in Europe and shared by other institutes, including INRIM (IT) and METAS (CH). A second transportable station will be devoted to calibration of the MWL time transfer system and comparison with the laser time transfer link ELT. As illustrated in Fig. 2, space-to-ground time comparisons will occur over four continents and will enable ground-to-ground comparisons over intercontinental scales. Combined with the growing network of continental links using compensated optical fibers that have already demonstrated frequency comparison capacity at $1{\cdot}10^{-19}$ resolution, clock frequency comparisons at the level of $1{\cdot}10^{-17}$ or better will soon be available with ACES on a worldwide scale. This represents a one to two orders of magnitude improvement over the currently used and widespread GPS time transfer system. These institutes are equipped with microwave fountain clocks operating with cesium or rubidium atoms as well as clocks operating in the optical domain. Fountain clocks are mature instruments and run with very high duty cycle (>95%) and will be compared over the whole ACES mission duration with the space clocks. Triggered by advances in laser cooling and trapping of atoms and ions, and by frequency comparisons using frequency combs [18,19], optical clocks have also made spectacular advances in the last years [20,21] with stability at 1 s of $3{\cdot}10^{-16}$ averaging down to $2{\cdot}10^{-18}$ after 20 000 s, [22–24], see also other reports in this dossier. These clocks are not yet as reliable as microwave fountain clocks but, with ACES, these optical clocks will be compared on intercontinental scales with 10^{-17} fractional frequency resolution during dedicated sessions. These record figures open new opportunities for testing fundamental laws of physics through comparisons between clocks of different types, and for probing the Earth's gravitational potential by comparing clocks in different locations.

4. The cold atom cesium clock PHARAO

Microwave clocks operating with laser-cooled cesium atoms in atomic fountains are today used to realize the unit of time, the second, with the best accuracy [25,26,30]. About ten of these devices are operating continuously and report their accuracy to BIPM for the realization of the International Atomic Time and UTC, the Universal Coordinate Time [34]. The fountain clock relative frequency stability is in the range $2\text{–}15{\cdot}10^{-14}\ \tau^{-1/2}$, where τ is the averaging time in seconds, reaching $1{\cdot}10^{-16}$ after a few days of integration [25]. Reported accuracies to BIPM are also in the $2\text{–}3{\cdot}10^{-16}$ range [26,16].

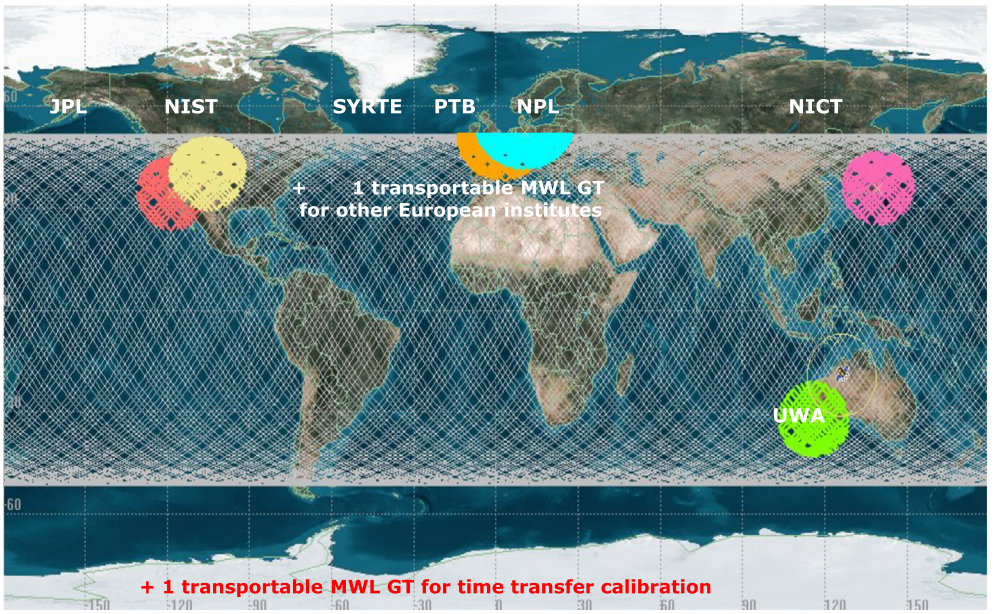

Fig. 2. (Color online.) The current network of seven ground institutes participating to the ACES mission and typical trajectories of the International Space Station. A transportable ground terminal will be available for additional European institutes and a second transportable terminal for global time transfer calibrations.

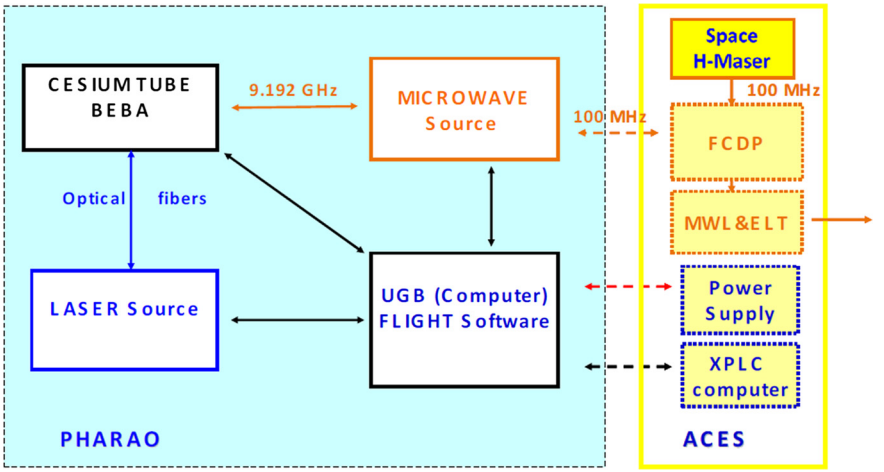

Fig. 3. (Color online.) PHARAO sub-systems and interfaces with the other elements of the ACES payload.

The PHARAO clock is a laser-cooled microwave cesium clock designed for micro-gravity operation [5,17]. It will realize in space a primary frequency standard where the very slow speed of the atoms in the device will enhance the resonance quality factor and reduce several systematic frequency shifts that occur in Earth-based fountains. The frequency stability target in space environment is $1{\cdot}10^{-13}\ \tau^{-1/2}$, with an accuracy of $1\text{–}2{\cdot}10^{-16}$. The overall mass and power consumption of PHARAO is 90 kg and 110 W for an overall length of 990 mm.

4.1. Architecture

The PHARAO clock main elements and interfaces are depicted in Fig. 3. It comprises four main elements, the cesium tube, the microwave source, the laser source and the computer with its dedicated software. Interfaces with the ACES payload include 100 MHz input and output signals to the Frequency Comparison and Distribution Package (FCDP), and connections to the power supply and ACES computer. Each element has been designed, developed, and tested independently before overall assembly and tests at CNES Toulouse premises. The cesium tube and laser source have been realized by SODERN, the microwave source by THALES, and the computer by EREMS. All sub-systems have passed the qualification tests for flight: storage temperature −40, +40 °C, random vibration level 10 g_{rms} in 200 Hz bandwidth, and 30 g at 30 Hz frequency.

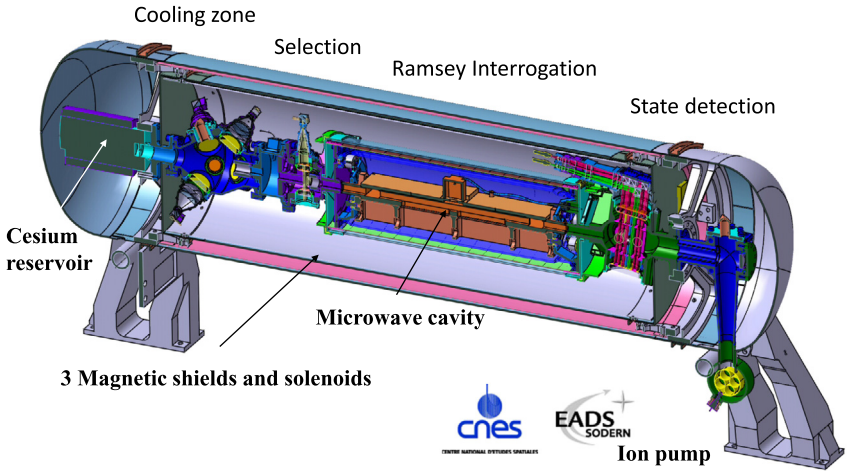

Fig. 4. (Color online.) The cesium tube. The overall length is 990 mm for a weight of 45 kg. Realization by Sodern.

4.2. Cesium tube

Cesium atoms are manipulated inside a non-magnetic titanium vacuum chamber in an UHV environment maintained by an ion pump and five getter materials (see Fig. 4).

The various titanium parts are connected using flexible gaskets in order to sustain thermal and mechanical stress during thermal cycling of the instrument (-40, $+40\,^{\circ}$C), outgassing at $+140\,^{\circ}$C, and mechanical vibrations. The residual pressure is 10^{-10} Torr and is sufficient for the slow propagation of the cloud of cold atoms through the tube with no appreciable atom loss by collisions with the residual gas. A reservoir retains cesium atoms in a matrix of titanium micro-balls. When the reservoir is heated, an atomic beam is produced, and an adjustable flux of atoms enters the capture region, where six laser beams with 10.5 mm waist and 13 mW power intersect to create the optical molasses. Atoms are captured and cooled in a few hundred milliseconds, then launched along the tube axis, and cooled to 1 μK. Through the frequency difference of the molasses beams during launch, the velocity of the atomic cloud can be adjusted between 5 cm/s and 5 m/s. The cloud diameter is 20 mm. After launch, 98.6% of the atoms are in the $F = 4$ hyperfine level of the cesium ground state with a balanced population among the nine Zeeman m_F sub-levels. Atoms then enter a preparation cavity where a microwave field selectively transfers atoms from $|F = 4, m_F = 0\rangle$ to $|F = 3, m_F = 0\rangle$. A transverse laser beam then pushes away atoms that remained in all m_F Zeeman states of $F = 4$. The atomic cloud is thus in a nearly pure quantum state $|F = 3, m_F = 0\rangle$ with 99% purity with 1% residuals in other Zeeman sub-states. For probing the magnetic field along the propagation direction of the tube, atoms from $|F = 4, m_F = 0\rangle$ can be transferred to the magnetically sensitive state $|F = 3, m_F = 1\rangle$ in the preparation cavity. Furthermore, slightly upstream from the pushing beam, a pulsed laser beam allows one to transfer part of the atoms from $|F = 3, m_F = 0\rangle$ to $|F = 4\rangle$ before they are pushed away, enabling slicing of the atomic cloud to improve the spatial localization of the atoms along the cesium tube. This improves the spatial resolution of the magnetic field map measured by the atoms during propagation and operation with very slow launch velocities.

Atoms then enter a microwave cavity where they experience the two-pulse Ramsey interrogation sequence. The distance between the two excitation regions is 200 mm, corresponding for the slowest launch velocity of 5 cm/s to a Ramsey dark period of 4 s and a resonance width of 0.12 Hz. The fastest launch velocity of 5 m/s provides a width of 12 Hz. This tunability enables us to evaluate systematic frequency shifts associated with the atom's velocity over two orders of magnitude, a feature that is not available in atomic fountains. After the Ramsey interrogation, atoms are detected in a state-selective manner by four successive and spatially separated laser beams with rectangular shape (5×14 mm) and circular polarization. The beams are tilted by 8 deg from normal incidence to reduce the fluorescence signal emitted by the residual thermal atoms propagating along the tube through a (small) Doppler frequency shift. The first beam is a standing wave tuned to the cycling $|g, F = 4, m_F = 4\rangle$ to $|e, F' = 5, m'_F = 5\rangle$ optical transition. The fluorescence emitted by the atoms is collected with a large aperture lens and focused on a photodiode, providing an overall detection efficiency of 5%. This fluorescence signal is proportional to the number of atoms transferred in $F = 4$ by the microwave interactions. The second beam is a traveling wave that deflects away the previously detected atoms. The third beam repumps the $F = 3$ atoms into the $F = 4$ state. The fourth beam, in a standing wave configuration, is identical to the first beam and now counts $F = 3$ atoms by the fluorescence collected on a second photodiode. This procedure allows us to count both atoms in the $F = 3$ and the $F = 4$ states and to compute the transition probability $N_4/(N_3 + N_4)$ with high signal-to-noise ratio, in a way similar to that achieved in atomic fountains.

As atomic energy levels are sensitive to stray electric and magnetic fields, much care has been taken to reduce their effect to a level compatible with 10^{-16} accuracy. DC stark shifts are eliminated by using metallic materials properly grounded. AC stark shift induced by the coupling to black-body radiation has been carefully evaluated by extensive thermal simulations, optimized design to reduce temperature gradients, and calibrated thermal probes with 0.05-K accuracy. Microwave leakages

Fig. 5. (Color online.) The PHARAO microwave source. From an ultra-stable 5 MHz quartz oscillator the microwave source generates a low noise and tunable 9.192 GHz signal for probing the cesium hyperfine structure. Realization by Thales.

are vastly reduced by waveguide cut-offs around the microwave interaction zones and metallic optical collimators mounts on the windows of the vacuum chamber with RF ring isolators. A homogeneous bias magnetic field of order 1 mG is applied along the tube using solenoid coils surrounding the microwave cavity and preparation regions. Three layers of magnetic shields improve the magnetic field homogeneity and attenuates by 18 000 external fields [27]. As this passive isolation is not sufficient in space, an active compensation system with a magnetic probe located inside the outmost magnetic shield and a servo-loop driving a current in a long solenoid provides a further attenuation by a factor 15 [28].

4.3. Microwave source

Designed and manufactured by Thales, the microwave source provides the 9.2-GHz microwave signals that feed the preparation cavity and the Ramsey cavity (Fig. 5). These signals are synthesized in two steps. The first one starts with a 5-MHz ultra stable quartz oscillator, which is frequency multiplied to generate a tunable 100 MHz signal split in two outputs. One is the PHARAO frequency output, which is sent to the onboard phase comparator FCDP for a phase comparison with the 100 MHz provided by the hydrogen maser. The FCDP output steers the PHARAO 100 MHz on the H-maser signal using a phase-locked loop and a Direct Digital Synthesizer (DDS). The relative frequency resolution is $8.5{\cdot}10^{-16}$ Hz. The second stage starts with a 100-MHz input (coming either from the first stage or from an external source) to synthesize by frequency multiplication and phase-locked loops the two 9.2 GHz signals, one for the state-preparation cavity, one for the Ramsey interaction cavity. A second DDS tunes the frequency with a resolution of 118 nHz. The output power levels can be adjusted over a 60-dB dynamic range with 0.02 dB steps to cover all possible atomic interaction times spanning two orders of magnitude. A switch with 80 dB attenuation turns off the state preparation microwave signal. In normal operation the Ramsey interaction signal is always turned on to avoid phase transient effects. The important characteristics of the microwave source are the low phase-noise level (-63 dBrad^2/Hz at 1 Hz) and the high spectral purity of the 9.2 GHz signal. The phase-noise contributes to the clock frequency stability, while the absence of spurious lines leads to no significant frequency shift of the atomic resonance. The PHARAO microwave source has been tested at SYRTE with the atomic fountain FO1 and the measured stability, was $7{\cdot}10^{-14}\,\tau^{-1/2}$ from 1 to $2{\cdot}10^5$ seconds. The PHARAO computer commands the microwave source operation during the clock cycles.

4.4. Laser source

Designed and manufactured by Sodern company, the laser bench provides the 10 laser beams required to cool, launch, state select, and detect the atoms in the cesium tube. The beams are transmitted to the cesium tube device through polarization maintaining fibers. All beam powers are measured at fiber exits and power-stabilized by the computer. The laser source consists of a double-sided optical bench with integrated control electronics, as shown in Fig. 6. The volume is 7 L for a weight of 21 kg. The optical bench is regulated at a temperature of 26 °C degrees within 0.2 °C. This maintains the beam alignments in the whole operating temperature range of the clock $[+10, +33]$ °C. Two extended cavity diode lasers (ECDL) (each with a back-up for redundancy) are locked to cesium lines in small glass cells with a frequency stability of about 100 kHz. One ECDL phase locks two 150 mW slave diode lasers (also with back-ups) by optical injection to provide enough laser power for fast loading of cold atoms in optical molasses. Six acousto-optic modulators allow fine frequency tuning and laser power control. Mechanical shutters provide complete extinction of the laser beams during Ramsey interaction preventing light shifts. The laser beam injection into each fiber is optimized by using a mirror mounted on miniature piezoelectric translators. The operation of the laser source is controlled by the computer to run the successive phases of atomic manipulation during one clock cycle: capture, launch, cooling, atomic cloud slicing, state selection, and detection. A specificity of the laser source is the high level of compactness and integration with hundreds of optical components and thousands of screws enabling optical alignment stability after space qualifications, vibrations at 100 m/s^2 and temperature cycling from -40, to $+40$ °C. Important parameters of the laser source are the laser power to load a large number of cold atoms, a low relative intensity noise and low phase noise to reach the lowest atomic temperature and to detect the atoms with high signal-to-noise ratio, contributing to the clock short-term stability [29].

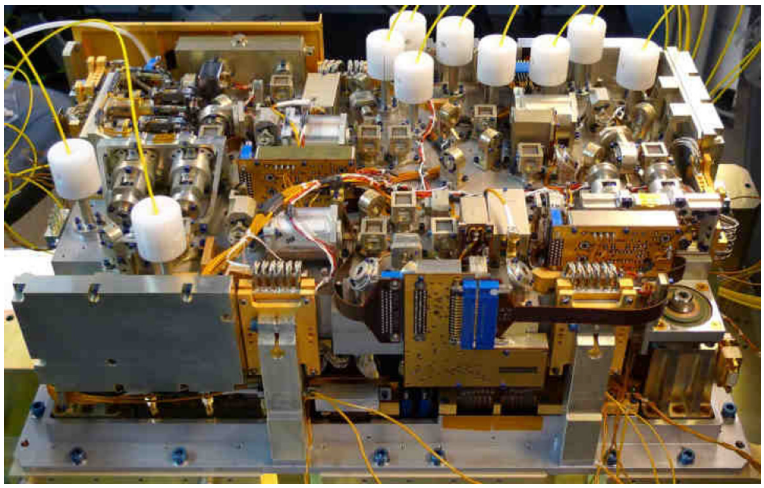

Fig. 6. (Color online.) The laser source. It includes 8 frequency stabilized semiconductor diode lasers. Volume is 7 L and mass, including electronics, is 21 kg. Realized by Sodern.

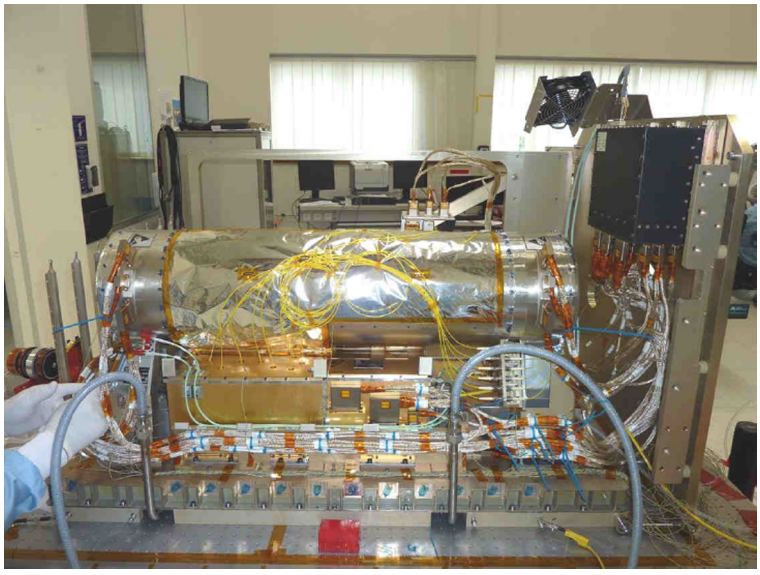

Fig. 7. (Color online.) The complete PHARAO clock mounted on the ACES baseplate.

4.5. Computer and software

Realized by EREMS, the PHARAO computer is the link with the ground operation center via data exchange with the ACES payload computer XPLC. It configures and receives data through serial lines from all PHARAO sub-systems and regulates their operation by using 22 programmable timers. The computer also drives all thermal and magnetic regulations. Through analog-digital converters, it acquires several physical measurements in real time, including the fluorescence signals in the detection regions. The software is organized in sequences ($\sim$100) and each sequence corresponds to a particular task or configuration: to turn on/off, to enable diagnostics, and to operate the clock in a large range of parameters. A list of sequences can be automatically processed from the off-state to full clock operation. About 500 parameters and 1000 timetables have been established to study and optimize the PHARAO operation in various conditions. The ACES ground segment controls the clock by sending telecommands, and by receiving data, which are processed, displayed, and stored in the ACES data base.

4.6. Tests on ground

All PHARAO sub-systems have passed the qualification tests: random vibration level $10\,g_{\mathrm{rms}}$, 30 g at 50 Hz, storage temperature -40, $+40\,^{\circ}$C, operating temperature $+10, +33\,^{\circ}$C. Fig. 7 shows the final assembly of PHARAO on the ACES baseplate at CNES Toulouse premises. During clock performance tests on ground the cesium tube is aligned vertically and

Fig. 8. (Color online.) Tests of PHARAO in the vacuum chamber at CNES. Note the large coils around the chamber to simulate the variations of the magnetic field in Earth orbit. In changing environmental conditions (temperature and magnetic field) the number of detected atoms remained stable within 1%.

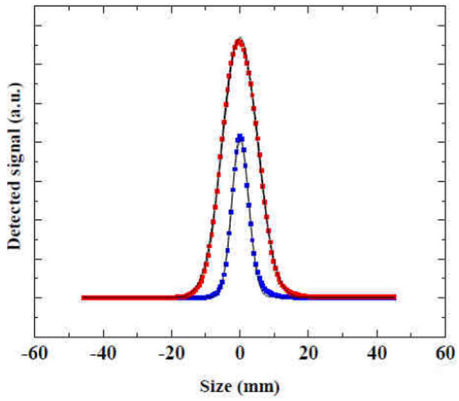

Fig. 9. (Color online.) Fluorescence signal in the detection zone without (red) and with slicing procedure of the atomic cloud (blue). Solid lines are Gaussian fits with waists of 10.1 mm and 5 mm, respectively. In clock operation, this signal is sampled, digitized by the computer (solid points), and integrated to derive the atom number in each one of the cesium hyperfine levels. Scanning the microwave frequency thus provides the transition probability between hyperfine states as a function of microwave detuning. (For interpretation of the references to color in this caption, the reader is referred to the online version of this article.)

atoms are launched upwards at a velocity of 3.56 m/s. The clock is operating under vacuum (see Fig. 8). Space environment is simulated by inducing variations of the baseplate temperature and of an applied magnetic field using large external Helmholtz coils to emulate the Earth's magnetic field changes in orbit (± 40 μT over 5400 seconds). The ground clock performance tests lasted 4 months, and ended in summer 2014. The capture, cooling, launch, and detection of cold atoms have been tested and optimized. The frequency stability and the largest systematic frequency shifts of the clock have also been measured. A short summary of the main results are given below.

The typical number of atoms loaded in optical molasses is $5{\cdot}10^8$ for a laser power of 13 mW/beam and a loading time of 1.5 s. During ground operation, we reduce this number to about $5{\cdot}10^7$ (laser power 5 mW/beam, loading time 200 ms) to avoid saturation of the fluorescence signals in the detection zone. Fig. 9 shows the time-dependent atomic fluorescence signal in the detection laser beam and converted in position space by means of the launch velocity. The fluorescence profile illustrates the typical initial molasses size without or with slicing of the atomic cloud. The molasses density distribution is fitted with a Gaussian distribution with $1/e^2$ width of 10.1 mm and 5 mm, respectively. In a microgravity environment, this slicing technique will be used to map the longitudinal magnetic field distribution in the clock and to detect density-dependent frequency shifts in the low launch velocity regime.

When the frequency of the 9.2-GHz microwave field is scanned around the cesium hyperfine frequency, the transition probability displays the Ramsey resonance pattern shown in Fig. 10. The line shape is in full agreement with the simulation that takes into account different interaction times in the first and second Ramsey zones because of atom slowing when propagating upwards in the Earth's gravity field. The central fringe line width is 5.6 Hz, which corresponds to an interaction time on the ground of 90 ms. In micro-gravity, this linewidth can be reduced to reach 0.12 Hz, with a launch velocity of 50 mm/s. During clock operation on the ground, the microwave frequency is modulated from cycle to cycle by half the fringe width, ± 2.8 Hz, in order to lock the local oscillator to the resonance frequency of the central fringe.

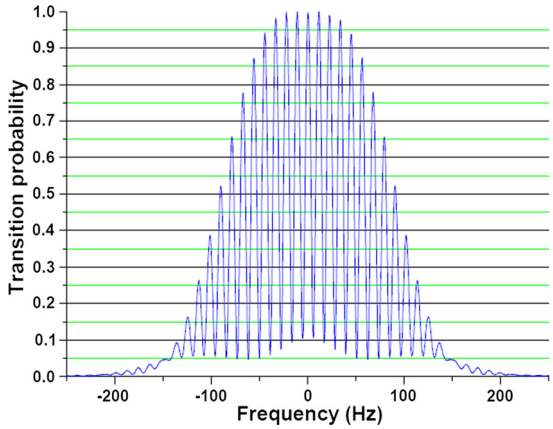

Fig. 10. (Color online.) Transition probability as a function of microwave detuning of the PHARAO clock near 9.192631770 GHz. On ground, the width of the Ramsey resonance is 5.6 Hz and limited by the Earth gravity.

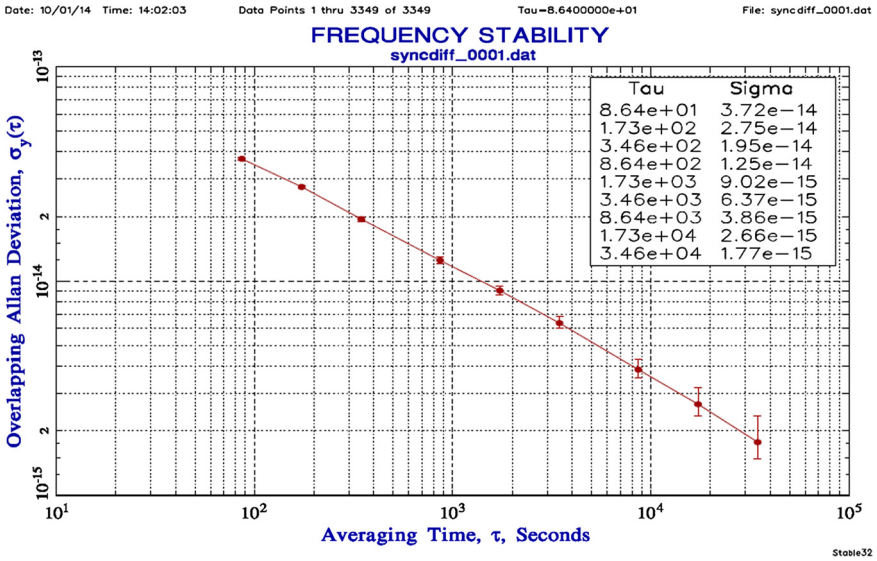

Fig. 11. (Color online.) PHARAO frequency stability on the ground measured against the mobile cold atom fountain FOM. The stability averages down as $3.4{\cdot}10^{-13}\,\tau^{-1/2}$ where τ is the measurement time in seconds.

Fig. 11 shows the measured frequency stability of PHARAO on the ground as a function of integration time τ, in seconds, when PHARAO is compared with the SYRTE mobile cesium fountain FOM [26]. The frequency stability is $3.4{\cdot}10^{-13}\tau^{-1/2}$, where the PHARAO contribution is $3.15{\cdot}10^{-13}\tau^{-1/2}$ and FOM contribution is $1.3{\cdot}10^{-13}\tau^{-1/2}$. The measured PHARAO stability is fully consistent with our simulation model, which takes into account the different sources of noise. Our clock model predicts that a frequency stability of $1.1{\cdot}10^{-13}\tau^{-1/2}$ can be achieved during microgravity operation when the resonance width will be reduced by one order of magnitude or more. The expected frequency stability in space is mostly dominated by the quartz oscillator noise of $8{\cdot}10^{-14}$ between 0.1 and 10 s, even if this oscillator displays one of the lowest reported phase noises. Cryogenic oscillators at GHz frequencies [31] or divided optical frequencies [32] would enable PHARAO to operate at $\sim 6{\cdot}10^{-14}$ at 1 s, but these instruments still remain to be space qualified. Our simulation also shows that the quality of the microgravity environment onboard the satellite is an important element for reaching the lowest frequency instability, especially for the longest interaction times [33].

The frequency accuracy of the PHARAO clock has been analyzed and systematic frequency shifts are summarized in Table 1. The dominant frequency shift results from the applied magnetic field. Fig. 12 shows the Ramsey resonance obtained by using the hyperfine transition between $m = 1$ Zeeman sub-levels. This transition is $\sim 10^7$ times more sensitive to the magnetic field than the $\Delta m = 0$ transition used during clock operation. The high-contrast Ramsey profile illustrates that the magnetic field experienced by the atoms is very homogeneous along the atomic path ($\delta B/B \sim 10^{-3}$, with $B = 1$ mG). In flight, the variation (± 40 μT) of the Earth field along the ISS orbit is an important issue as the overall shielding factor of 270,000 is not sufficient to totally cancel its effect. Clock frequency variations of about $2{\cdot}10^{-16}$ will remain. We correct this effect by periodically measuring the magnetic field experienced by the atoms at a rate of 2 mHz by using the high

Table 1
Main systematic frequency shifts and uncertainties in PHARAO ground tests.

Effect	Correction (10^{-15})	Uncertainty (10^{-16})
Magnetic field	181	<1
Black-body shift	−17.6	<1
Collisions	−7	12
Longitudinal phase gradient	3	6
Microwave recoil/lensing	0.12	<1
Phase transients	<1	<1
Total	160.55	14

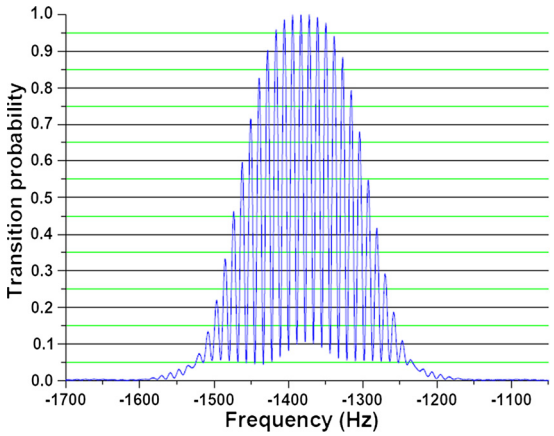

Fig. 12. (Color online.) Transition probability on an $m = 1 \rightarrow m' = 1$ Zeeman sensitive transition as a function of microwave detuning of the PHARAO clock, referenced to 9.192631770 GHz.

sensitivity of the $m = 1$ hyperfine resonance. The measurement lasts only 10 s and will have negligible influence on the overall clock stability measurement. We expect a final uncertainty close to 10^{-17} for the magnetic field residual uncertainty.

The second main systematic effect is the black-body radiation shift [36]. The thermal configuration of the cesium tube has been carefully modeled using finite-element analysis. The model has been tested using calibrated platinum resistors located in several key places along the cesium tube. From this analysis, we infer an uncertainty on the absolute temperature seen by the atoms in the interaction region of 56 mK, which gives a $1.5{\cdot}10^{-17}$ contribution for the black-body shift uncertainty. The third effect results from atomic collisions. For cold cesium atoms, the frequency shift depends on the relative energy of the colliding atoms in a non-trivial manner and on the local density. First, this shift is made relatively small by using optical molasses as a source rather than a magneto-optical trap. Second, it is measured by operating the clock with different atom numbers and densities, comparing the clock frequencies and extrapolating to the zero-density limit. Third, for long interrogation times achievable in micro-gravity, the atomic density can be made small. The number of atoms is varied by changing the frequency of the preparation cavity with optimized power. In these conditions, our model predicts that the local atomic density follows the same reduction as the atom number to better than 1%. A summary of the main frequency shifts with their uncertainties measured on the ground is given in Table 1. On the ground, the uncertainty was mainly limited by the measurement duration. In space, due to the energy dependence of the frequency shift, the collisional shift will vary as a function of the launch velocity. In typical operation with a velocity of 300 mm/s, we predict a frequency shift of $1.5{\cdot}10^{-15}$. This shift can even cancel for a velocity of 150 mm/s. Measurements will be performed during the whole mission duration to reach an uncertainty of $5{\cdot}10^{-17}$. The fourth important effect is the residual Doppler effect resulting from the inhomogeneous phase distribution of the microwave field inside the cavity. This distribution has been calculated by numerical simulations and verified by measurements. On the ground, the longitudinal phase gradient is amplified due to the atomic deceleration between the first and the second Ramsey interactions and we compute a frequency shift of $3{\cdot}10^{-15}$. In space, the same calculation gives $3{\cdot}10^{-17}$ for typical operating conditions. This effect is linear with the atomic velocity, but is coupled with the collisional shift. In space, by varying both the launch velocity, and density over two orders of magnitude, we expect an uncertainty of $5{\cdot}10^{-17}$ for the combined effect. The effect of the transverse phase gradient in an unperfect cavity is currently under investigation in a collaboration with K. Gibble [39,16]. Among all other small effects, the recoil shift with microwave photons or microwave lensing effect remains to be analyzed in greater depth [40]. The effect is of the order of $1{\cdot}10^{-16}$, but the exact value depends on the initial atom's wave function size and on the geometry of the cesium tube.

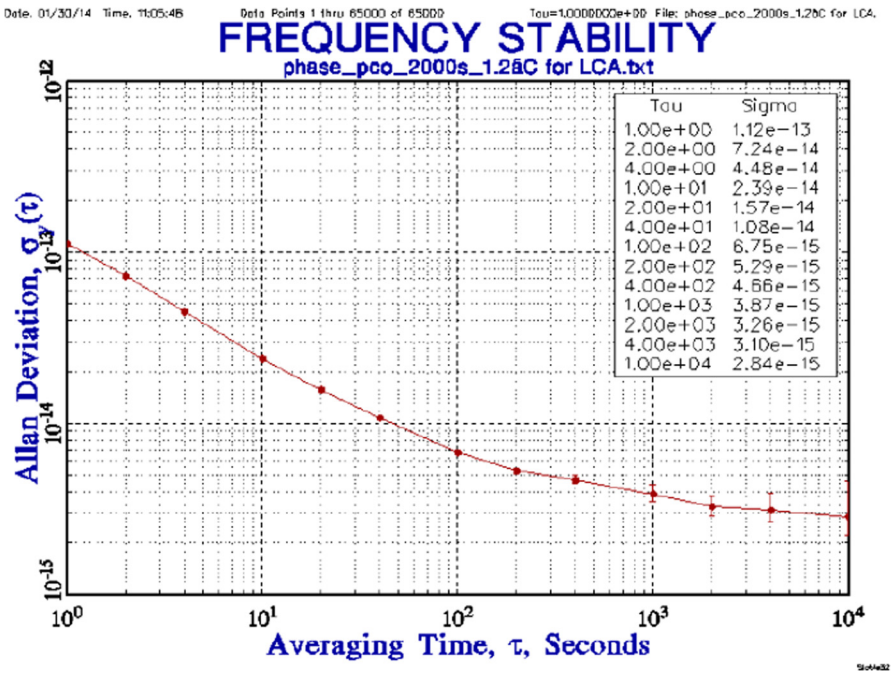

Fig. 13. (Color online.) Frequency stability of the SHM engineering model with a baseplate temperature modulation of ±0.6 K over a period of 2000 s. The SHM stability is measured against an unperturbed hydrogen maser at SpectraTime.

5. The Space Hydrogen Maser

The Space Hydrogen Maser (SHM) is an active maser developed by SpectraTime (CH) since 2009 [41]. To fit low mass (45 kg) and volume constraints, the core of the maser uses a glass bulb surrounded by an aluminum microwave cavity tuned to the 1.420405751 GHz hydrogen hyperfine frequency and enclosed in five layers of magnetic shields. SHM is attached to the ACES base plate whose temperature is actively regulated to within ±0.65 °C. A dedicated Automatic Cavity Tuning system (ACT) has been developed to maintain the microwave cavity tuned to resonance, thus correcting for temperature drifts. In stable thermal and magnetic conditions, the engineering model of SHM displays the frequency stability reported in Fig. 13 that lies very close to the specifications. However, tests have revealed a non-conformance with the specifications for the thermal sensitivity and, more importantly, for the magnetic sensitivity coefficients. The thermal sensitivity can be counter-acted by a faster servo of the base plate temperature (period shorter than 600 s) and by the natural filtering of fluctuations by the thermal inertia of the maser structure. More serious is the magnetic field sensitivity coefficient of $4{\cdot}10^{-14}$/Gauss, which is about four times above the specified value. The typical magnetic field variations on orbit of ±40 μT are expected to degrade the SHM frequency stability to about $1{\cdot}10^{-14}$ at half the orbital period, i.e. 2700 s. Improvements are under study and tests will be performed on a modified version of the SHM engineering model with a thicker external magnetic shield. This modification and other improvements in the magnetic shield design are expected to reduce the SHM magnetic sensitivity to an acceptable level. The flight model delivery is currently expected at the end of 2015, as the last element to be mounted on the ACES baseplate.

6. The microwave time transfer system

The ACES clock signal is compared to ground clocks by the ACES microwave link, MWL, developed by TimeTech and ADS [35]. The MWL uses a two-way time transfer system [38] with a carrier frequency in the Ku-band, 13.5 GHz and 14.7 GHz for the up- and down-link respectively. The two-way configuration is mandatory to remove tropospheric and ionospheric time delays and achieve cancellation of the first-order Doppler effect. In comparison with the *S* band, the high carrier frequencies of the Ku-band signals enable an important reduction of the ionospheric time delay. An additional down-link in *S*-band (2.2 GHz) is used to determine precisely the Total Electron Content (TEC) and correct for the ionospheric delay. A PN-code modulation (100 Mchip/s) of the carrier removes the phase ambiguity between successive comparison sessions separated by dead times corresponding to one or several orbital periods. The system allows for four simultaneous ground users distinguished by different Doppler shifts and PN-codes. This capacity of simultaneous comparisons is particularly useful in Europe due to the high density of national metrology institutes.

End-to-end tests of the MWL engineering model performances have been successfully completed in May 2014. The sub-picosecond phase resolution at 300 s, corresponding to a typical ISS path duration above a given ground station, has been demonstrated as well as a long-term stability well below 5 ps. The MWL flight model is under construction with

a number of design improvements, which have been identified during the tests, on software, DDS, and space qualified electronics. The flight model is expected to be delivered to ADS in October 2015 for final performance tests in end-to-end configuration and integration on the ACES platform.

7. The laser time transfer system

The laser time transfer ELT (European Laser Timing) has been proposed by the University of Prague and the Technical University of Munich [42] as an alternative time transfer link. Picosecond laser pulses from ground-based satellite laser ranging stations are fired towards the ACES platform, detected by an avalanche photodiode on board and time tagged in the ACES time scale. Part of the laser beam is reflected back to ground by a corner-cube reflector, enabling precise ranging and removal of tropospheric effects in the comparison of time scales. ELT is an extension of the T2L2 time transfer experiment currently running on the JASON2 satellite [43] with, however, an important difference. Whereas T2L2 operates with laser pulses leading to the onboard detection of several tens to hundred photons, ELT operates in single photon counting mode. This has the advantage of removing the complex calibration of the avalanche photodiode time delay, which depends in a non-linear manner on the impinging laser intensity, at the expense, however, of a reduced signal-to-noise ratio at short measurement times. Nevertheless, analysis and tests performed at the Wetzell laser ranging station have shown that excellent performance can still be achieved, at the level of a few ps per ISS path and less than 7 ps over several days. The latter value is comparable to the MWL specification at 10 days. The flight model of ELT detector is close to completion and the timing unit will soon be integrated in the MWL electronic board. Participation of the laser ranging stations to the ELT time transfer experiment will be organized by the ELT data center (Technical University of Munich) in the frame of the International Laser Ranging Service (ILRS).

8. ACES operations and ground segment

The ACES Users Support and Operations Center (USOC) will be located at CADMOS, in CNES Toulouse. It will operate the payload via the Columbus Control Center and operate remotely the MWL ground terminals connected to a set of ground based microwave and optical clocks (see Section 3). The ground segment architecture has been designed and first tests of its operation have been completed. The USOC will send commands and receive telemetry, collect, and store scientific data. The data will be analyzed by the data analysis center located at the Paris Observatory which will provide higher level data products to the scientific community. They include space to ground clock de-synchronization, correction of known systematic effects in various instruments, orbit determination of the ACES payload, ranging measurements, and atmospheric delays. The complete set of raw data will be stored and made available for post-processing, subsequent refinements of the data analysis, and distribution to the wider scientific community. The ACES mission life time is nominally 18 months with possible extension to 36 months. The first six months will be dedicated to the in-flight characterization of the space clocks, the microwave time transfer link, the optical link, and the orbit determination via GPS/GNSS. After this phase, the optimal configuration for PHARAO and SHM will be established. ACES will then enter its nominal mode of operation characterized by a very stable configuration. This will enable long-term comparisons of the ACES signal with ground clocks, full characterization of the PHARAO clock frequency stability and accuracy, and ground-to-ground clock long-term comparisons on a worldwide basis.

9. Perspectives

This report gave a brief overview of the recent activities on the ACES mission. The next two years will be devoted to the integration and tests of the remaining ACES elements before launch, currently planned for the first half of 2017. In parallel, the microwave link terminals will be installed at the participating ground institutes and tested with the whole ACES ground segment (operations, communications, data exchange and storage). The preparation for data analysis is well advanced and will also be a central element for the success of the ACES mission. ACES will represent a key step in the demonstration of cold-atom-based quantum devices and sensors for space applications. Second-generation missions, such as STE–QUEST aiming at testing the Equivalence Principle in Space, are presently under study [44] and partly described in this volume [37].

A number of modern physical theories attempt to unify gravity with the other three fundamental interactions well described by the Standard Model of particle physics. They include string theory, super-string theory, and M-theory. In many of these theories, new particles and fields are predicted, which may couple with regular matter. In scenarios like the runaway Dilaton model of Damour, Piazza, and Veneziano [45], fundamental physical constants, such as the fine structure constant or the electron to proton mass ratio, are no longer “constant”, but evolve with time, and the Einstein Equivalence Principle is violated at some level. Therefore, precision tests of the gravitational redshift and the search for a possible drift of fundamental constants, as planned in the ACES mission, and Equivalence Principle tests, as planned in the MICROSCOPE mission [46] and STE–QUEST [44], will either set new, tighter constraints on these new particles and their coupling to matter, or uncover new physical effects. The quest for more and more precise tests of the fundamental laws of physics remains a fascinating goal!

Acknowledgements

The development of the ACES mission is a collective effort and the authors would like to thank all participants, in particular the ACES Investigator working group (IWG), the ACES project team at ESA, ADS, TimeTech, the PHARAO team at CNES, LNE-SYRTE and LKB, the PHARAO industrial team at TAS, Sodern, Erems, CS, the SHM team at SpectraTime, the University of Prague team, the Technical University Munich team, and the data analysis team at LNE-SYRTE, NPL and PTB for their crucial contributions to the ACES mission. This work is supported by ESA, CNES, and CNRS.

References

[1] P.R. Berman (Ed.), Atom Interferometry, Academic Press, 1997.
[2] A.D. Cronin, J. Schmiedmayer, D.E. Pritchard, Rev. Mod. Phys. 81 (2009) 1051.
[3] C.J. Bordé, Metrologia 39 (2002) 1339.
[4] B. Lounis, J. Reichel, C. Salomon, C. R. Acad. Sci. Paris, Ser. II 316 (1993) 739–744.
[5] P. Laurent, P. Lemonde, E. Simon, G. Santarelli, A. Clairon, P. Petit, N. Dimarcq, C. Audoin, C. Salomon, Eur. Phys. J. D 3 (1998) 201.
[6] R. Geiger, V. Menoret, G. Stern, N. Zahzam, P. Cheinet, B. Battelier, A. Villing, F. Moron, M. Lours, Y. Bidel, A. Bresson, A. Landragin, P. Bouyer, Nat. Commun. 2 (2012) 474.
[7] T.v. Zoest, N. Gaaloul, Y. Singh, H. Ahlers, W. Herr, S.T. Seidel, W. Ertmer, E. Rasel, M. Eckart, E. Kajari, S. Arnold, G. Nandi, R. Walser, W.P. Schleich, A. Vogel, K. Sengstock, K. Bongs, W. Lewoczko-Adamczyk, M. Schiemangk, A. Peters, T. Könemann, Science 328 (2010) 1540–1543, http://dx.doi.org/10.1126/science.1189164.
[8] S. Dickerson, J. Hogan, A. Sugarbaker, D. Johnson, M. Kasevich, Phys. Rev. Lett. 111 (2013) 083001.
[9] H. Müntiga, et al., Phys. Rev. Lett. 110 (2013) 093602.
[10] E. Simon, P. Laurent, G. Santarelli, A. Clairon, P. Lemonde, C. Salomon, N. Dimarcq, P. Petit, C. Audoin, F. Gonzalez, F. Jamin-Changeart, Acta Astron. 12 (1997) 837.
[11] V.A. Kostelecky, C.D. Lane, Phys. Rev. D 60 (1999) 116010.
[12] C. Salomon, N. Dimarcq, M. Abgrall, A. Clairon, P. Laurent, P. Lemonde, G. Santarelli, P. Uhrich, L.G. Bernier, G. Busca, A. Jornod, P. Thomann, E. Samain, P. Wolf, F. Gonzalez, P. Guillemot, S. Leon, F. Nouel, C. Sirmain, S. Feltham, C. R. Acad. Sci. Paris Sér. IV Phys. Astrophys. 2 (2001) 1313.
[13] C. Salomon, L. Cacciapuoti, N. Dimarcq, Int. J. Mod. Phys. D 16 (2007) 2511.
[14] L. Cacciapuoti, N. Dimarcq, G. Santarelli, P. Laurent, P. Lemonde, A. Clairon, P. Berthoud, A. Jornod, F. Reina, S. Feltham, C. Salomon, Nucl. Phys. B, Proc. Suppl. 166 (2007) 303.
[15] Luigi Cacciapuoti, Christophe Salomon, Space clocks and fundamental tests: the ACES experiment, Eur. Phys. J. Spec. Top. 172 (2009) 57.
[16] R. Li, K. Gibble, K. Szymaniec, Metrologia 48 (2011) 283.
[17] P. Laurent, M. Abgrall, I. Moric, P. Lemonde, G. Santarelli, A. Clairon, S. Bize, D. Rovera, J. Guéna, C. Salomon, M. Aubourg, F. Picard, P. Chatard, S. Léon, C. Sirmain, D. Massonnet, O. Grosjean, C. Delaroche, J.-F. Végua, N. Ladiette, M. Chaubet, B. Léger, C.-M. De Graeve, S. Julien, M. Saccoccio, D. Blonde, B. Faure, A. Ratsimandresy, S. Béraud, F. Buffe, I. Zenone, P. Larivière, C. Escandes, B. Vivian, C. Luitot, F. Gonzalez, J.-P. Granier, P. Guillemot, C. Macé, S. Thomin, J.-P. Lelay, T. Potier, Y. Cossart, T. Nauleau, A. Granget, Rev. Fr. Métrol. 34 (2) (2014).
[18] S.A. Diddams, et al., Phys. Rev. Lett. 84 (2000) 5102.
[19] R. Holzwarth, et al., Phys. Rev. Lett. 85 (2000) 2264.
[20] T. Rosenband, et al., Science 319 (2008) 1808.
[21] A.D. Ludlow, et al., Science 319 (2008) 1805.
[22] N. Hinkley, et al., Science 341 (2013) 1215.
[23] B.J. Bloom, et al., Nature 506 (2014) 71.
[24] I. Ushijima, et al., ArXiv, arXiv:1405.1471, 2014.
[25] S. Bize, P. Laurent, M. Abgrall, H. Marion, I. Maksimovic, L. Cacciapuoti, J. Grünert, C. Vian, F. Pereira dos Santos, P. Rosenbusch, P. Lemonde, G. Santarelli, P. Wolf, A. Clairon, A. Luiten, M. Tobar, C. Salomon, J. Phys. B, At. Mol. Opt. Phys. 38 (2005) S449–S468.
[26] J. Guéna, M. Abgrall, D. Rovera, P. Laurent, B. Chupin, M. Lours, G. Santarelli, P. Rosenbusch, M.E. Tobar, R. Li, K. Gibble, A. Clairon, S. Bize, IEEE Trans. Ultrason. Ferroelectr. Freq. Control 59 (2012) 391.
[27] I. Moric, Ph. Laurent, Ph. Chatard, S. Thomin, V. Christophe, O. Grosjean, Acta Astron. 102 (2014) 287.
[28] I. Moric, C. De Graeve, O. Grosjean, Ph. Laurent, Rev. Sci. Instrum. 85 (2014) 075117.
[29] T. Leveque, B. Faure, F.X. Esnault, C. Delaroche, D. Massonnet, O. Grosjean, F. Buffe, P. Torresi, T. Bomer, A. Pichon, P. Beraud, J.-P. Lelay, S. Thomin, Ph. Laurent, Rev. Sci. Instrum. (2015), submitted for publication.
[30] M. Abgrall, et al., C. R. Physique 16 (2015) 461–470, this issue.
[31] A.G. Mann, S. Chang, A.N. Luiten, IEEE Trans. Instrum. Meas. 50 (2001) 519.
[32] J. Millo, M. Abgrall, M. Lours, E. English, H. Jiang, J. Guéna, A. Clairon, M. Tobar, S. Bize, Y. Le Coq, G. Santarelli, Appl. Phys. Lett. 94 (2009) 141105.
[33] P. Lemonde, PhD thesis, Paris-6 University, 1997.
[34] G. Petit, F. Arias, G. Panfilo, C. R. Physique 16 (2015) 480–488, this issue.
[35] M.-P. Hess, L. Stringhetti, B. Hummelsberger, K. Hausner, R. Stalford, R. Nasca, L. Cacciapuoti, R. Much, S. Feltham, T. Vudali, B. Leger, F. Picard, D. Massonnet, P. Rochat, D. Goujon, W. Schaefer, P. Laurent, P. Lemonde, A. Clairon, P. Wolf, C. Salomon, I. Prochazka, U. Schreiber, O. Montenbruck, Acta Astron. 69 (2011) 929.
[36] W. Itano, L. Lewis, D. Wineland, Phys. Rev. A 25 (1981) 1233.
[37] C. Guerlin, P. Delva, P. Wolf, C. R. Physique 16 (2015) 565–575, this issue.
[38] R.F.C. Vessot, et al., M.W. Levin, F.E.M. Mattison, E.L. Blomberg, T.E. Hoffman, G.U. Nystrom, B.F. Farrell, R. Decher, P.B. Eby, C.R. Baugher, J.W. Watts, D.L. Teuber, F.D. Wills, Phys. Rev. Lett. 45 (December 1980) 2081.
[39] J. Guéna, R. Li, K. Gibble, S. Bize, A. Clairon, Phys. Rev. Lett. 106 (2011) 130801.
[40] K. Gibble, Phys. Rev. A 90 (2014) 015601.
[41] D. Goujon, P. Rochat, P. Mosset, D. Boving, A. Perri, J. Rochat, N. Ramanan, D. Simonet, X. Vernez, S. Froidevaux, G. Perruchoud, in: Proc. of the 24th European Frequency and Time Forum, 2010.
[42] J. Blazej, I. Prochazka, J. Kodet, P. Linhart, in: 3rd Annual Conference on Laser Communication and Propagation through the Atmosphere and Oceans, in: Proceedings of SPIE, vol. 9224, 2014, p. 978.
[43] E. Samain, P. Vrancken, P. Guillemot, P. Fridelance, P. Exertier, Metrologia 51 (2014) 503.
[44] P. Wolf, et al., submitted to the European Space Agency in answer to the M4 mission call, January 2015.
[45] T. Damour, F. Piazza, G. Veneziano, Phys. Rev. Lett. 89 (2002) 081601.
[46] P. Touboul, G. Métris, V. Lebat, A. Robert, Class. Quantum Gravity 89 (2012) 184010.